

# EXPONENTIAL POLYNOMIAL TIME INTEGRATORS \*

TOMMASO BUVOLI<sup>†</sup>

**Abstract.** In this paper we extend the polynomial time integration framework to include exponential integration for both partitioned and unpartitioned initial value problems. We then demonstrate its utility by constructing a new class of parallel exponential block methods based on the Legendre points. These new integrators can be constructed at arbitrary orders of accuracy, have improved stability compared to existing polynomial based exponential linear multistep methods, and can offer significant computational savings compared to current state-of-the-art methods.

**Key words.** Time-integration, polynomial interpolation, general linear methods, parallelism, high-order.

**AMS subject classifications.** 65L04, 65L05, 65L06, 65L07

Polynomial time integrators [3, 6] are a class of parametrized methods for solving first-order systems of ordinary differential equations. The integrators are based on a new framework that combines ideas from complex analysis, approximation theory, and general linear methods. The framework encompasses all general linear methods that compute their outputs and stages using interpolating polynomials in the complex time plane. The use of polynomials enables one to trivially satisfy order conditions and easily construct a range of implicit or explicit integrators with properties such as parallelism and high-order of accuracy.

In order to extend the utility of the polynomial framework, we generalize it to include exponential integration. Exponential integrators are a general class of methods that incorporate exponential functions to provide increased stability and accuracy for solving stiff systems [19]. Continuing efforts to construct and analyze exponential integrators have already produced a wide range of methods [2, 8, 22, 24, 17, 18, 23, 19, 33] that can provide improved efficiency compared to fully implicit and semi-implicit integrators [15, 22, 26, 30]. However, incorporating parallelism into exponential integrators remains an open question. Typically, parallelism is applied within an exponential scheme to speed up the estimation of exponential matrix functions and their products with vectors; examples include parallel Krylov projections [27] and parallel rational approximations of exponential functions [16, 37, 38]. To the best of our knowledge there has only been limited research in developing exponential integrators that naturally incorporate parallelism in their stages and outputs. Exponential EPIRK methods with independent stages [35] and parallel exponential Rosenbrock methods [28] constitute exceptions to this assessment. However, both of these approaches are limited since they require a restricted integrator formulation that only permits a limited number of stages to be parallelized. Furthermore, it is difficult to derive arbitrary-order parallel schemes of this type.

In this work we extend the polynomial framework to include exponential integration, and then demonstrate several key advantages of this approach by constructing new, parallel, high-order exponential polynomial block methods. We then compare this approach to existing exponential integrators that can also be implemented at high-orders of accuracy.

---

\*Submitted to the editors DATE.

**Funding:** This work was funded by the National Science Foundation, Computational Mathematics Program, under DMS-1115978 and DMS-1216732

<sup>†</sup>Department of Applied Mathematics, University of Washington, Seattle, WA USA. (bu-voli@uw.edu).

This paper is organized as follows. In Sections 1 and 2 we provide a brief introduction to polynomial methods and exponential integrators. In Sections 3 and 4 we extend the framework to include exponential integration, and then describe some general strategies for constructing polynomial block methods. We also introduce a new class of polynomial block methods based on the Legendre points. Next, in Section 5, we analyze and compare the stability regions of the new methods compared to existing exponential Adams-Bashforth and exponential Runge-Kutta methods. Finally, in Section 6, we perform numerical experiments comparing EPBMS to a variety of other high-order exponential integrators.

**1. Polynomial time integrators.** Polynomial time integrators [3, 6] are a general class of parametrized methods constructed using interpolating polynomials in the complex time plane. The polynomial framework is based on the *ODE polynomial* and the *ODE dataset*. The former describes a range of polynomial-based approximations, and the later contains the data values for constructing these interpolants. The primary distinguishing feature of a polynomial method is that each of its stages and outputs are computed by evaluating an ODE polynomial. In the subsections below we begin by briefly reviewing the ODE dataset, the ODE polynomial, and the notation used to describe polynomial time integrators. We then extend the definition to include exponential integration, introduce exponential polynomial block methods (EPBMs) and discuss several construction strategies.

**1.1. The ODE dataset.** The ODE dataset is an ordered set containing all possible data values for constructing the interpolating polynomials that are used to compute a method's outputs. At the  $n$ th timestep an ODE dataset contains a method's inputs, outputs, and stage values along with their derivatives and their temporal nodes. The data is represented in the local coordinates  $\tau$  where the global time is

$$(1.1) \quad t = r\tau + t_n,$$

and  $r$  is a scaling factor. An ODE dataset of size  $w$  is represented with the notation  $D(r, t_n) = \{(\tau_j, y_j, rf_j)\}_{j=1}^w$  where  $y_j \approx y(t(\tau_j))$ , and  $f_j = F(t(\tau_j), y_j)$ .

**1.2. The ODE polynomial.** An ODE polynomial can be used to represent a wide variety of approximations for the Taylor series of a differential equation solution. In its most general form, an ODE polynomial of degree  $g$  with expansion point  $b$  is

$$(1.2) \quad p(\tau; b) = \sum_{j=0}^g \frac{a_j(b)(\tau - b)^j}{j!}$$

where each approximate derivative  $a_j(b)$  is computed by differentiating interpolating polynomials constructed from the values in an ODE dataset

$$D(r, t_n) = \{(\tau_j, y_j, rf_j)\}_{j=1}^w.$$

For details regarding the most general formulations for the approximate derivatives  $a_j(b)$  we refer the reader to [3, 6]. *Adams ODE polynomials* are one special family of ODE polynomials that are related to this work. Every Adams ODE polynomial can be written as

$$(1.3) \quad p(\tau; b) = L_y(b) + \int_b^\tau L_F(\xi) d\xi$$

where  $L_y(\tau)$  and  $L_F(\tau)$  are Lagrange interpolating polynomials that respectively approximate  $y(t)$  and its derivative  $ry'(t)$ . These polynomials can be used to construct classical Adams-Bashforth methods and their generalized block counterparts from [6].

**1.3. Parameters and notation for polynomial methods.** During the timestep from  $t_n$  to  $t_{n+1} = t_n + h$ , a polynomial method accepts inputs  $y_j^{[n]}$  and produces outputs  $y_j^{[n+1]}$  where  $j = 1, \dots, q$ . Every input and output of a polynomial method approximates the differential equation solution  $y(t)$  at a particular time. In local coordinates we represent these time-points using the node set  $\{z_j\}_{j=1}^q$  such that

$$y_j^{[n]} \approx y(t_n + rz_j) \quad \text{and} \quad y_j^{[n+1]} \approx y(t_n + rz_j + h).$$

The input nodes of a polynomial method scale with respect to the *node radius*  $r$ , which is independent of the stepsize  $h = r\alpha$ . The parameter  $\alpha$  is known as the *extrapolation factor* and its value signifies the number of node radii per timestep. In general, polynomial methods are described in terms of  $r$  and  $\alpha$  rather than  $r$  and  $h$  since these are natural variables for working with polynomials in local coordinates.

A polynomial method with  $s$  stages and  $q$  outputs can be written as

$$\begin{aligned} Y_i &= p_j(c_j(\alpha), b_j(\alpha)) & j &= 1, \dots, s, \\ y_j^{[n+1]} &= p_{j+s}(z_j + \alpha; b_{j+s}(\alpha)) & j &= 1, \dots, q, \end{aligned}$$

where  $Y_i$  denote stage values and  $p_j(\tau; b)$  are all ODE polynomials constructed from an ODE dataset containing the methods inputs, outputs, and stage values.

**1.3.1. Propagators and iterators.** We distinguish between two important types of polynomial methods: propagators and iterators. Propagators advance the solution forward in time and are characterized by an extrapolation factor  $\alpha$  that is greater than zero. When  $\alpha$  is zero, the stepsize  $h = r\alpha = 0$ , and the method reduces to an iterator that recomputes the solution at the current time-step. In Figure 1 we provide a visualization for these two types of methods.

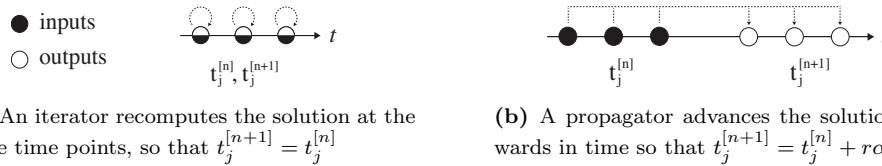


**Fig. 1:** Iterator and propagator methods. Input times  $t_j^{[n]}$  and output times  $t_j^{[n+1]}$  are shown on the real  $t$  line when  $z_j$  are three equispaced points. Iterators can be useful for correcting or updating an approximate solution, while propagators are traditional time-stepping schemes.

**2. Exponential integrators.** Exponential integrators are a class of numerical methods for solving stiff initial value problems [19]. They are derived from the prototypical semilinear equation

$$(2.1) \quad \mathbf{y}' = \mathbf{L}\mathbf{y} + N(t, \mathbf{y}), \quad \mathbf{y}(t_0) = \mathbf{y}_0,$$

where the linear operator  $\mathbf{L}$  and the nonlinear operator  $N(t, \mathbf{y})$  are chosen so that they approximate the original ODE problem. In practice the linear operator  $\mathbf{L}$  is selected so that it captures the majority of the stiffness of the right-hand side.

The exact solution to (2.1) is obtained by applying the discrete variation of constants formula to obtain the integral equation

$$(2.2) \quad \mathbf{y}(t) = e^{(t-t_0)\mathbf{L}}\mathbf{y}(t_n) + \int_{t_n}^t e^{(t-s)\mathbf{L}}N(s, \mathbf{y}(s))ds.$$

Exponential integrators treat the linear term  $\mathbf{L}$  exactly while approximating the nonlinearity  $N(s, y(s))$  with a polynomial. For example, the 2nd-order exponential Runge-Kutta ETD RK2 from [8]

$$(2.3) \quad \begin{aligned} Y_1 &= e^{h\mathbf{L}}y_n + \int_0^1 e^{(1-s)h\mathbf{L}}N(t_n, y_n) \\ y_{n+1} &= e^{h\mathbf{L}}y_n + \int_0^1 e^{(1-s)h\mathbf{L}} [N(t_n, y_n) + s(N(t_{n+1}, Y_1) - N(t_n, y_n))] \end{aligned}$$

utilizes polynomials that are constructed using stage values. Similarly, the 2nd-order exponential Adams-Bashforth method [2, 8]

$$(2.4) \quad y_{n+1} = e^{h\mathbf{L}}y_n + h \int_0^1 e^{(1-s)h\mathbf{L}} [N(t_n, y_n) + s(N(t_n, y_n) - N(t_{n-1}, y_{n-1}))] ds$$

utilizes a Lagrange interpolating polynomial constructed using previous solution values. Since exponential integrators involve weighted integrals of polynomials and exponentials, they are frequently expressed in terms of the  $\varphi$ -functions

$$(2.5) \quad \varphi_n(z) = \begin{cases} e^z & n = 0, \\ \frac{1}{(n-1)!} \int_0^1 e^{z(1-s)} s^{n-1} ds & n > 0. \end{cases}$$

Using this notation the Adams-Bashforth method (2.4) can be written as

$$y_{n+1} = \varphi_0(hL)y_n + \varphi_1(hL)hN(t_n, y_n) + \varphi_2(hL)h(N(t_n, y_n) - N(t_{n-1}, y_{n-1})).$$

**2.1. Unpartitioned exponential integrators.** Exponential integrators like (2.3) and (2.4) are known as *partitioned exponential integrators* [8, 2, 34] since they can only be applied to the partitioned semilinear problem (2.1). *Unpartitioned* exponential integrators [35, 40, 41] have also been developed for solving the more general initial value problem

$$(2.6) \quad \mathbf{y}' = F(t, \mathbf{y}), \quad \mathbf{y}(t_0) = \mathbf{y}_0.$$

The key intuition is that one may obtain a localized semi-linear problem of the form (2.1) at  $t = t_n$  by rewriting the system in its autonomous form  $\mathbf{y}' = F(\mathbf{y})$  and then rewriting  $F(\mathbf{y})$  as

$$(2.7) \quad \begin{aligned} F(\mathbf{y}) &= F(\mathbf{y}_n) + \mathbf{J}_n(\mathbf{y} - \mathbf{y}_n) + R(\mathbf{y}) \\ R(\mathbf{y}) &= F(\mathbf{y}) - [F(\mathbf{y}_n) + \mathbf{J}_n(\mathbf{y} - \mathbf{y}_n)] \end{aligned}$$

where  $\mathbf{y}_n = \mathbf{y}(t_n)$  and  $\mathbf{J}_n = \frac{\partial F}{\partial \mathbf{y}}(\mathbf{y}(t_n))$  is the Jacobian of  $\mathbf{y}(t)$  at  $t = t_n$ . The linear operator  $\mathbf{J}_n$  takes the place of  $\mathbf{L}$  in (2.1) and the remaining terms form the nonlinearity. Given the initial condition  $\mathbf{y}(t_n) = \mathbf{y}_n$ , the solution of (2.6) is

$$(2.8) \quad \mathbf{y}(t) = e^{(t-t_n)\mathbf{J}_n}\mathbf{y}_n + \int_{t_n}^t e^{(t-s)\mathbf{J}_n} [F(\mathbf{y}_n) - \mathbf{J}_n \mathbf{y}_n + R(\mathbf{y})] ds.$$

Depending on the approximation that is chosen for the remainder term  $R(\mathbf{y})$  one arrives at different families of unpartitioned exponential integrators [35, 40, 41].

**3. Exponential polynomial methods.** To introduce polynomial-based exponential integrators we first extend the definitions of the ODE dataset and the ODE polynomial. We then replace the ODE polynomials in classical polynomial integrators with these generalized approximations. In each of the following subsections we begin by presenting a general formulation of a concept and then describe a special sub-case with a reduced number of free parameters. Since the space of exponential polynomial methods is very large, each of these subfamilies are aimed at simplifying the initial construction of new integrators.

**3.1. ODE dataset and ODE polynomial.** We first generalize the ODE dataset and ODE polynomial for the partitioned initial value problem (2.1). We can trivially extend the ODE datasets by replacing full derivatives with the nonlinear derivative component  $N(t, \mathbf{y}(t))$ .

DEFINITION 3.1 (Exponential ODE Dataset). *An exponential ODE dataset  $D(r, s)$  of size  $w$  is an ordered set of tuples*

$$(3.1) \quad D(r, s) = \{(\tau_j, \mathbf{y}_j, r\mathbf{N}_j)\}_{j=1}^w$$

where  $t(\tau) = r\tau + s$ ,  $\mathbf{y}_j \approx \mathbf{y}(t(\tau_j))$ , and  $\mathbf{N}_j = N(t(\tau_j), \mathbf{y}_j)$ .

Next we introduce a new ODE polynomial that approximates the truncated Taylor series for the local solution  $N(t(\tau), \mathbf{y}(\tau))$ , expanded around the point  $\tau = b$ .

DEFINITION 3.2 (ODE Derivative Component Polynomial). *An exponential ODE derivative component polynomial of degree  $g$  is a polynomial of the form*

$$(3.2) \quad \dot{p}(\tau; b) = \sum_{j=0}^g \frac{a_j(b)(\tau - b)^j}{j!}$$

where the approximate derivative

$$a_j(b) = \left. \frac{d^j}{d\tau^j} l_j(\tau) \right|_{\tau=b}.$$

and  $l_j(\tau)$  is a polynomial of lowest degree that interpolates at least one nonlinear derivative component value in the ODE dataset  $D(r, s)$ . We may express the conditions on  $l_j(\tau)$  mathematically as

$$l_j(\tau_k) = r\mathbf{N}_k \quad \text{for} \quad k \in \mathcal{C}^j$$

where  $\mathcal{C}^j$  is a set that contains unique indices ranging from 1 to  $w$ .

A classical polynomial integrator utilizes ODE polynomials to approximate the solution. To develop exponential integrators we generalize this concept by introducing a new approximation based on the integral equation (2.2). We begin by rewriting the ODE in local coordinates  $\tau$  where  $t(\tau) = r\tau + t_n$  and assume that we are provided with an initial condition at  $\tau = \tau_0$ . We then apply the integrating factor to obtain the exact solution and consider the following approximation:

$$(3.3) \quad \mathbf{y}(\tau) = e^{r\mathbf{L}(\tau-\tau_0)} \underbrace{\mathbf{y}(\tau_0)}_{\substack{\text{Approximate using a} \\ \text{classical ODE Polynomial}}} + \int_{\tau_0}^{\tau} e^{\mathbf{L}r(\tau-s)} \overbrace{r\mathbf{N}(s, \mathbf{y}(s))}^{\substack{\text{Approximate using an ODE} \\ \text{derivative component polynomial}}} ds.$$

We name an approximation of this form a polynomial  $\varphi$ -expansion since it can be expressed as a linear combination of  $\varphi$ -functions (2.5) with weights that depend on the approximate derivatives of the two ODE polynomials. Every polynomial  $\varphi$ -expansion depends on three parameters: the expansion points of the ODE polynomial and ODE derivative component polynomial, and the left integration point  $\tau_0$ . We will respectively refer to these three parameters  $b_1$ ,  $b_2$  and  $b_3$  and use the symbol  $\psi(\tau; b_1, b_2, b_3)$  to represent a polynomial  $\varphi$ -expansion.

**DEFINITION 3.3 (Polynomial  $\varphi$ -Expansion).** *Let  $\dot{p}(\tau; b_2)$  be an ODE derivative component polynomial of degree  $g$  with approximate derivatives  $a_j(b_2)$ , and let  $p(\tau; b_1)$  be an ODE polynomial. A polynomial  $\varphi$ -expansion  $\psi(\tau; b_1, b_2, b_3)$  approximates the local solution  $y(t(\tau))$  and has three equivalent representations:*

1. *The integral formulation:*

$$(3.4) \quad \psi(\tau; b_1, b_2, b_3) = e^{r\mathbf{L}(t-b_3)} \underbrace{p(b_3; b_1)}_{\substack{\text{Classical ODE polynomial for } y(t) \\ \text{expanded at } b_3 \text{ and evaluated at } b_1.}} + \int_{b_3}^{\tau} e^{r\mathbf{L}(\tau-s)} \overbrace{\dot{p}(s; b_2)}^{\substack{\text{ODE derivative component polynomial for } N(\tau, y(\tau)) \\ \text{expanded at } b_2}} ds.$$

2. *The differential formulation:  $\psi(\tau; b_1, b_2, b_3)$  is the solution of the linear system*

$$(3.5) \quad \begin{aligned} \mathbf{y}'(\tau) &= r\mathbf{L}\mathbf{y} + \dot{p}(\tau; b_2), \\ \mathbf{y}(b_3) &= p(b_3; b_1). \end{aligned}$$

3. *The  $\varphi$ -expansion formulation:*

$$(3.6) \quad \begin{aligned} \psi(\tau; b_1, b_2, b_3) &= \varphi_0(r\mathbf{L}(\tau - b_3))p(b_1; b_3) + (\tau - b_3) \sum_{k=0}^g \mathbf{c}_k(\tau) \varphi_{k+1}(r\mathbf{L}(\tau - b_3)) \\ \mathbf{c}_k(\tau) &= \sum_{j=k}^g \frac{a_j(b_2)(\tau - b_3)^j (b_3 - b_2)^{j-k}}{(j-k)!}. \end{aligned}$$

We demonstrate the equivalence of these three representations in appendix A.

A polynomial  $\varphi$ -expansion has many free parameters. To simplify method construction, we introduce a special family of polynomial  $\varphi$ -expansions that is related to the Adams ODE polynomial (1.3) for classical integrators.

**DEFINITION 3.4 (Adams  $\varphi$ -Expansion).** *The polynomial  $\varphi$ -expansion (3.4, 3.5, 3.6) is of Adams type if it satisfies the following two conditions:*

1. *The ODE polynomial  $p(\tau; b_1) = L_y(\tau)$  where  $L_y(\tau)$  is a Lagrange interpolating polynomial that interpolates at least one solution value in an ODE dataset.*
2. *The ODE derivative component polynomial  $\dot{p}(\tau; b_2) = L_N(\tau)$  where  $L_N(\tau)$  is a Lagrange interpolating polynomial that interpolates any number of derivative component values in an ODE dataset.*

The Lagrange polynomials  $p(\tau; b_1)$  and  $\dot{p}(\tau; b_2)$  that make up an Adams  $\varphi$ -expansion do not depend on their expansion points. Therefore we may express the  $\varphi$ -expansion in terms of a single parameter  $b$ . The three representations are

1. integral  $\psi(\tau; b) = e^{r\mathbf{L}(t-b)} L_y(b) + \int_b^{\tau} e^{r\mathbf{L}(\tau-s)} L_N(s) ds,$
2. differential  $\mathbf{y}'(\tau) = r\mathbf{L}\mathbf{y} + L_N(\tau), \quad \mathbf{y}(b) = L_y(b),$
3.  $\varphi$ -expansion  $\psi(\tau; b) = \varphi_0(r\mathbf{L}(\tau - b)) L_y(b) + \sum_{k=0}^g (\tau - b)^{k+1} L_N^{(k)}(b) \varphi_{k+1}(r\mathbf{L}(\tau - b)).$

We name these simplified  $\varphi$ -expansions Adams  $\varphi$ -expansions for two reasons. First they reduce to a classical Adams ODE polynomial (1.3) as  $\mathbf{L} \rightarrow \mathbf{0}$ . Second, we can derive exponential Adams-Bashforth and Adams-Moulton methods [2] using an Adams  $\varphi$ -expansion constructed from an ODE dataset with equispaced nodes.

**3.1.1. Obtaining coefficients for polynomial  $\varphi$ -expansions.** From the integral formulation (3.6) we see that all polynomial  $\varphi$ -expansions are linear combinations of  $\varphi$ -functions where the weights are expressed in terms of:

1. the ODE polynomial  $p(\tau; b_1)$  evaluated at  $\tau = b$ ,
2. the approximate derivatives  $a_j(b)$  of the derivative ODE polynomial  $\dot{p}(\tau; b_2)$ .

These two quantities can each be represented as linear combinations of the data elements in the ODE dataset that were used to form  $p(\tau; b_2)$  and  $\dot{p}(\tau; b_2)$ . A detailed procedure for obtaining these weights is described in [3, Sec 3.7]. Note that the procedure for computing the approximate derivatives of  $\dot{p}(\tau; b_2)$  is identical to the one for an ODE polynomial with approximate derivatives that are obtained by differentiating a polynomial approximation to  $y'(t(\tau))$ .

For Adams  $\varphi$ -expansions, the procedure for obtaining coefficients is simpler. To rewrite an Adams  $\varphi$ -expansion as a linear combination of  $\varphi$ -functions, one must rewrite  $L_y(b)$  and  $L_N^{(k)}(b)$  in terms of the values and derivatives in the ODE dataset that were used to form the Lagrange interpolating polynomials  $L_y(\tau)$  and  $L_N(\tau)$ . In other words, we must find the coefficients  $a_j$  and  $c_{\nu,j}$  so that

$$(3.7) \quad L_y(b) = \sum_{j=1}^w a_j \mathbf{y}_j \quad \text{and} \quad L_N^{(\nu)}(b) = \sum_{j=1}^w c_{\nu,j} r \mathbf{N}_j.$$

If  $\mathbf{y}_k$  is not used to form  $L_y(\tau)$ , then  $a_k$  is zero. Similarly, if  $r \mathbf{N}_k$  was not used to form  $L_N(\tau)$ , then  $c_{\nu,k} = 0$ . All the non-zero  $a_j$  are finite difference weights for computing the zeroth derivative at  $\tau = b$  using data at the nodes of the Lagrange polynomials  $L_y(\tau)$ . Similarly, all the non-zero  $c_{\nu,j}$  are finite difference weights for computing the  $\nu$ th derivative at  $\tau = b$  using data at the nodes of the Lagrange polynomials  $L_N(\tau)$ .

In general, the  $j$ th coefficient  $d_{\nu,j}$  for computing the  $\nu$ th derivative at  $x = x_0$  of a Lagrange polynomial  $L(x)$  with nodes  $x_j$  and data  $\mathbf{g}_j$ ,  $j = 0, \dots, q$ , can be found by inverting the  $q \times q$  Vandermonde matrix  $\mathbf{V}_{i,j} = (x_i - x_0)^{j-1}$  and letting  $d_{\nu,j} = \nu! \mathbf{V}_{\nu+1,j}^{-1}$ . Since Vandermonde matrices can be ill-conditioned it is advantageous to use the fast, stable algorithm developed by Fornberg for computing finite difference weights [10, 11].

**3.1.2. Extension to unpartitioned problems.** We can also extend the ODE dataset and the ODE polynomial for the unpartitioned problem (2.6) using local linearization. To derive an unpartitioned polynomial  $\varphi$ -expansion we:

1. rewrite (2.6) in autonomous form,
2. locally linearize around  $\tau = \ell$  to obtain the equation (2.7) with  $\mathbf{y}_n \rightarrow \mathbf{y}(\ell)$  and  $\mathbf{J}_n \rightarrow \frac{\partial F}{\partial \mathbf{y}}(\mathbf{y}_\ell)$ ,
3. re-express the equation in local coordinates  $\tau$ ,
4. assume that the initial condition is supplied at  $\tau = \tau_0$ .

Using the integrating factor method, the corresponding solution is

$$(3.8) \quad \mathbf{y}(\tau) = e^{(\tau-\tau_0)r\mathbf{J}(\mathbf{y}_\ell)} \mathbf{y}_0 + r \int_{\tau_0}^{\tau} e^{(\tau-s)r\mathbf{J}(\mathbf{y}_\ell)} [F(\mathbf{y}_\ell) - \mathbf{J}(\mathbf{y}_\ell) \mathbf{y}_\ell + R(\mathbf{y})] ds,$$

where  $\mathbf{y}_0 = \mathbf{y}(\tau_0)$ ,  $\mathbf{y}_\ell = \mathbf{y}(\ell)$ , and  $\mathbf{J}(y) = \frac{\partial F}{\partial \mathbf{y}}(y)$  is the Jacobian of the right-hand-side evaluated at  $y$ . Next we introduce the *unpartitioned ODE dataset* for the remainder

term

$$(3.9) \quad D(r, s) = \{(\tau_j, \mathbf{y}_j, rR(\mathbf{y}_j))\}_{j=1}^w,$$

and an associated ODE derivative component polynomial that is defined identically to the ODE derivative component polynomial in Definition 3.2 except  $N(t, \mathbf{y})$  is now  $R(\mathbf{y})$ . We obtain the unpartitioned polynomial  $\varphi$ -expansion approximation by making the following replacements to (3.8):

$$(3.10) \quad \mathbf{y}_0 \rightarrow p_1(\tau_0; b_1), \quad \mathbf{y}_l \rightarrow p_2(\ell; b_2), \quad \text{and} \quad R(\mathbf{y}(s)) \rightarrow \dot{p}(s; b_3),$$

where  $p_1(s, b_1)$  and  $p_2(s, b_2)$  are classical ODE polynomial approximating  $y(s)$  and  $\dot{p}(s; b_3)$  is an ODE derivative component polynomial approximating  $R(\mathbf{y}(s))$ . The polynomial  $\varphi$ -expansion now depends on the expansion points of the three ODE polynomials, the linearization point  $\ell$ , and the left integration point  $\tau_0$ . If we label these parameters using  $b_1, b_2, b_3, b_4, b_5$ , then we can use the symbol  $\hat{\psi}(\tau; b_1, b_2, b_3, b_4, b_5)$  to represent an unpartitioned polynomial  $\varphi$ -expansion. Once again, we can limit the number of free parameters by introducing a special family of approximations.

**DEFINITION 3.5** (Unpartitioned Adams  $\varphi$ -Expansion). *Let  $L_y(\tau)$  and  $L_R(\tau)$  be two Lagrange interpolating polynomials constructed from the ODE dataset (3.9) such that  $L_y(\tau)$  interpolates at least one solution value, and  $L_R(\tau)$  interpolates at any number of derivative component values;*

$$L_y(\tau_k) = \mathbf{y}_k \text{ for } k \in \mathcal{A}, |\mathcal{A}| \geq 1 \quad \text{and} \quad L_R(\tau_j) = rN(\tau_k, \mathbf{y}_k) \text{ for } k \in \mathcal{B}.$$

An unpartitioned Adams  $\varphi$ -expansion is an approximation of the form (2.8, 3.10) where  $p(s; b_1) = p(s; b_2) = L_y(s)$ ,  $\dot{p}(s; b_2) = L_R(s)$  and the expansion point  $\ell$  and left integration point  $\tau_0$  are equal such that  $\tau_0 = \ell = b$ .

If we let  $\mathbf{J}_b = \frac{\partial F}{\partial \mathbf{y}}(L_y(b))$  then we can write the formula for an unpartitioned Adams polynomial  $\varphi$ -expansion in the usual three ways:

$$\text{differential} \quad \mathbf{y}'(\tau) = rF(L_y(b)) + r\mathbf{J}_b(\mathbf{y}(\tau) - L_y(b)) + L_R(\tau), \quad \mathbf{y}(b) = L_y(b),$$

$$\begin{aligned} \text{integral} \quad \hat{\psi}(\tau; b) &= e^{r\mathbf{L}(\tau-b)} L_y(b) + \int_b^\tau e^{(\tau-s)r\mathbf{J}_b} [rF(L_y(b)) - r\mathbf{J}_b L_y(b) + L_R(s)] ds, \\ &= L_y(b) + \int_b^\tau e^{(\tau-s)r\mathbf{J}_b} [rF(L_y(b)) + L_R(s)] ds, \end{aligned}$$

$$\begin{aligned} \varphi\text{-expansion} \quad \hat{\psi}(\tau; b) &= L_y(b) + (\tau - b)\varphi_1(r\mathbf{J}_b(\tau - b))rF(L_y(b)) \\ &\quad + \sum_{k=0}^g (\tau - b)^{k+1} L_R^{(k)}(b)\varphi_{k+1}(r\mathbf{J}_b(\tau - b)). \end{aligned}$$

In each formula the identity  $e^{h\mathbf{A}}\mathbf{x} = \mathbf{x} + h\varphi_1(h\mathbf{A})\mathbf{A}\mathbf{x}$  was used to write the second formula in the integral formulation and the  $\varphi$ -formulation.

**3.2. A general formulation for exponential polynomial methods.** The general formulation for a partitioned exponential polynomial method with  $s$  stages and  $q$  outputs is

$$\begin{aligned} Y_i &= \psi_j(c_j(\alpha); b_{1,j}(\alpha), b_{2,j}(\alpha), b_{3,j}(\alpha)) & j &= 1, \dots, s \\ y_j^{[n+1]} &= \psi_{j+s}(z_j + \alpha; b_{1,j+s}(\alpha), b_{2,j+s}(\alpha), b_{3,j+s}(\alpha)) & j &= 1, \dots, q \end{aligned}$$

where  $Y_i$  are stage values and the  $\psi_j(\tau; b)$  are partitioned polynomial  $\varphi$ -expansions constructed from an ODE dataset that contains the methods inputs, outputs, and stage values. The definition for an unpartitioned integrator is identical except we replace the polynomial  $\varphi$ -expansions  $\psi_j$  with unpartitioned polynomial  $\varphi$ -expansions  $\hat{\psi}_j$  that depend on the parameters  $b_1(\alpha), \dots, b_5(\alpha)$ .

The space of all exponential polynomial methods is large. Therefore, in this initial work we restrict ourselves to block methods [12, 14] with  $q$  outputs and no stages. This leads to a simplified method formulation that still possesses multiple inputs for easily constructing high-order polynomial approximations of the solution and the nonlinear derivative component. Moreover, we also only consider methods with Adams  $\varphi$ -expansions. We briefly introduce exponential polynomial block methods (EPBMs) below and then discuss their construction in the next section.

**3.2.1. Adams exponential polynomial block methods.** A partitioned Adams EPBM depends on the parameters:

$$\begin{array}{ll} q & \text{number of inputs/outputs} & \{z_j\}_{j=1}^q & \text{nodes, } z_j \in \mathbb{C}, |z_j| \leq 1 \\ r & \text{node radius, } r \geq 0 & \{b_j\}_{j=1}^q & \text{expansion points} \\ \alpha & \text{extrapolation factor} & & \end{array}$$

and can be written as

$$(3.11) \quad y_j^{[n+1]} = \psi_j(z_j + \alpha; b_j(\alpha)), \quad j = 1, \dots, q,$$

where each  $\psi_j(\tau; b)$  is an Adams  $\varphi$ -expansion built from the exponential ODE dataset

$$D(r, t_n) = \underbrace{\left\{ \left( z_j, \mathbf{y}_j^{[n]}, r\mathbf{N}_j^{[n]} \right) \right\}_{j=1}^q}_{\text{method inputs}} \cup \underbrace{\left\{ \left( z_j + \alpha, \mathbf{y}_j^{[n+1]}, r\mathbf{N}_j^{[n+1]} \right) \right\}_{j=1}^q}_{\text{method outputs}}.$$

We can also write any partitioned Adams EPBM in coefficient form as

$$\begin{aligned} y_j^{[n+1]} &= \varphi_0(\eta_j \mathbf{L}) \sum_{k=1}^q \left( A_{jk} \mathbf{y}_k^{[n]} + C_{jk} \mathbf{y}_k^{[n+1]} \right) \\ &\quad + r \sum_{k=1}^q \varphi_k(\eta_j \mathbf{L}) \sum_{l=1}^q \left( B_{jkl} \mathbf{N}_l^{[n]} + D_{jkl} \mathbf{N}_l^{[n+1]} \right) \end{aligned}$$

where  $\eta_j = (z_j + \alpha - b_j)$  and  $j = 1, \dots, q$ . Similarly we can write an unpartitioned Adams EPBM as

$$(3.12) \quad y_j^{[n+1]} = \hat{\psi}_j(z_n + \alpha; b_j(\alpha)), \quad j = 1, \dots, q,$$

or in its coefficient form

$$\begin{aligned} y_j^{[n+1]} &= \left( A_{jk} \mathbf{y}_k^{[n]} + C_{jk} \mathbf{y}_k^{[n+1]} \right) + \varphi_1(\eta_j \mathbf{J}_{b_j}) F \left( \sum_{k=1}^q \left( A_{jk} \mathbf{y}_k^{[n]} + C_{jk} \mathbf{y}_k^{[n+1]} \right) \right) \\ &\quad + r \sum_{k=1}^q \varphi_k(\eta_j \mathbf{J}_{b_j}) \sum_{l=1}^q \left( B_{jkl} \mathbf{R}_l^{[n]} + D_{jkl} \mathbf{R}_l^{[n+1]} \right). \end{aligned}$$

**4. Constructing exponential polynomial methods.** We now introduce several approaches for constructing EPBMs with Adams polynomial  $\varphi$ -expansions. We will derive several classes of new parallel and serial EPBMs and discuss a strategy for obtaining initial conditions by composing multiple iterator methods.

**4.1. Constructing EPBMs.** To simplify method construction for Adams EPBMs it is convenient to rewrite them in the integral form

Partitioned:

$$y_j^{[n+1]} = e^{r\mathbf{L}(t-b)} L_y^{[j]}(b_j) + \int_{b_j}^{z_j+\alpha} e^{r\mathbf{L}(\tau-s)} L_N^{[j]}(s) ds,$$

Unpartitioned:

$$y_j^{[n+1]} = L_y^{[j]}(b_j) + r\eta_j \varphi_1(r\eta_j \mathbf{J}_{b_j}) F(L_y^{[j]}(b_j)) + \int_{b_j}^{z_j+\alpha} e^{r\mathbf{J}_{b_j}(\tau-s)} L_R^{[j]}(s) ds,$$

where  $\eta_j = z_j + \alpha - b_j$  and  $j = 1, \dots, q$ . To construct these types of methods we must select: (1) a set of nodes  $\{z_j\}_{j=1}^q$  that determine the input and output times, (2) the Lagrange polynomials  $L_y^{[j]}$ ,  $L_N^{[j]}$  or  $L_y^{[j]}$ ,  $L_R^{[j]}$  that respectively interpolate values or derivatives at the input and output nodes, and (3) the integration endpoints  $b_j$ . In the following subsections we describe multiple strategies for selecting each of these parameters. However we note that the parameters for exponential methods can be selected in entirely different ways and in a different order than what is shown in this paper.

**4.1.1. Node selection.** Polynomial methods can be constructed using either real-valued or complex-valued nodes  $\{z_j\}_{j=1}^q$ . For fully implicit polynomial methods, imaginary nodes offer improved stability compared to real-valued nodes [6]. However, for exponential methods good stability properties can be obtained with real-valued nodes. Therefore in the remainder of this work we will assume that all nodes are real-valued, and that the nodes are normalized so they lie on the interval  $[-1, 1]$  and that they are ordered so that

$$z_1 < z_2 < \dots < z_q.$$

Finally, though it lies outside the scope of this paper, we note that it is simple to adapt the ideas presented here to imaginary nodes sets like the imaginary equispaced points used to construct the BAM and BBDF methods in [6].

**4.1.2. Selecting the polynomial  $L_y^{[j]}(\tau)$  and the endpoints  $b_j$ .** The polynomial  $L_y^{[j]}(\tau)$  approximates the initial condition for the integral equation (3.3) and (3.8). Since we are interested in constructing high-order parallel methods, we choose the highest-order polynomial that doesn't prevent parallelism. This choice is  $L_y^{[j]}(\tau) = L_y(\tau)$ , where  $L_y(\tau)$  is a Lagrange interpolating polynomial of order  $q - 1$  that interpolates through each of the methods inputs so that

$$(4.1) \quad L_y(z_j) = y_j^{[n]} \quad \text{for } j = 1, \dots, q.$$

To simplify things even further, we select the integration endpoints so that they are equal to any of the node values; in other words, there must exist an integer  $k(j)$  such that  $b_j = z_{k(j)}$  for  $j = 1, \dots, q$ . Under these assumptions, the formula for the  $j$ th output of an EPBM reduces to

$$\begin{aligned} \text{P:} \quad y_j^{[n+1]} &= e^{r\mathbf{L}(t-b)} y_{k(j)}^{[n]} + \int_{b_j}^{z_j+\alpha} e^{r\mathbf{L}(\tau-s)} L_N^{[j]}(s) ds, \\ \text{UP:} \quad y_j^{[n+1]} &= y_{k(j)}^{[n]} + r\eta_j \varphi_1(r\eta_j \mathbf{J}_{b_j}) F(y_{k(j)}^{[n]}) + \int_{b_j}^{z_j+\alpha} e^{r\mathbf{J}_{b_j}(\tau-s)} L_R^{[j]}(s) ds. \end{aligned}$$

**4.1.3. Selecting the polynomials  $L_N^{[j]}(\tau)$  and  $L_R^{[j]}(\tau)$ .** The Lagrange polynomials  $L_N^{[j]}(\tau)$  and  $L_R^{[j]}(\tau)$  respectively approximate the nonlinear terms in the integral equations (3.3) and (3.8). Here we propose three strategies for choosing these polynomials that lead to either parallel or serial methods. We first describe the motivation behind our choices, then we present formulas that are written in terms of sets that contain the indices of the input and output data used to form the Lagrange polynomials. Finally we present several stencils that graphically illustrate the temporal locations of the data used to form the polynomials if the nodes are chosen to be three equispaced points on the interval  $[-1, 1]$ .

Before describing our choices we introduce the *input index set*  $I(j)$  and the *output index set*  $O(j)$ . These sets describe which data is used to construct the Lagrange polynomial and are defined as

$$\begin{array}{ll} \text{partitioned:} & \text{unpartitioned:} \\ k \in I(j) \iff L_N^{[j]}(z_k) = N_k^{[n]} & k \in O(j) \iff L_R^{[j]}(z_k) = R_k^{[n+1]}. \end{array}$$

The order of the polynomials  $L_N^{[j]}(z_k)$  and  $L_R^{[j]}(z_k)$  is therefore  $|I(j)| + |O(j)| - 1$ .

Our three proposed strategies for the construction  $L_N^{[j]}(\tau)$  and  $L_R^{[j]}(\tau)$  are:

1. *Parallel maximal-fixed-cardinality- $\ell$*  (**PMFC $_\ell$** ): The Lagrange polynomial interpolates the nonlinear derivatives at all input nodes with index greater than or equal to  $\ell$ . The set  $O$  must be empty to retain parallelism.
2. *Serial maximal-variable-cardinality- $\ell$*  (**SMVC $_\ell$** ): The Lagrange polynomial interpolates the nonlinear derivatives at all input nodes and previously computed outputs with index greater than or equal to  $\ell$ . The cardinality of set  $O(j)$  grows as we add new information.
3. *Serial maximal-fixed-cardinality- $\ell$*  (**SMFC $_\ell$** ): The Lagrange polynomial interpolates the nonlinear derivatives at all previously computed outputs and some of the inputs with index greater than or equal to  $\ell$ . To keep the cardinality of  $I(j) \cup O(j)$  fixed for all  $j$ , we drop inputs in favor of more recently computed outputs.

The formulas for the three construction strategies are written in the Table 1. To help

|                               | $I(j)$ - input index set                         | $O(j)$ - output index set          |
|-------------------------------|--|------------------------------------|
| <b>PMFC<math>_\ell</math></b> | $\{\ell, \ell + 1, \dots, q\}$                   | $\{\}$                             |
| <b>SMFC<math>_\ell</math></b> | $\{\max(j, \ell), \max(j, \ell) + 1, \dots, q\}$ | $\{\ell, \ell + 1, \dots, j - 1\}$ |
| <b>SMVC<math>_\ell</math></b> | $\{\ell, \ell + 1, \dots, q\}$                   | $\{\ell, \ell + 1, \dots, j - 1\}$ |

**Table 1:** Formulas describing the input index sets  $I(h)$  and the output index sets  $O(j)$  for three construction strategies.

illustrate the formula we show several stencil-like diagrams in Figure 2 that reveal the data locations used to form the interpolating polynomials. Finally, implicit EPBMs can be created by taking  $O(j) \rightarrow O(j) \cup j$ , however such methods are outside the scope of this paper.

**4.2. Iterator methods for obtaining initial conditions.** EPBMs require multiple inputs at the first time-step. Since we are normally provided with only one initial value, an exponential Runge-Kutta scheme can be used to compute the solution at each of the starting nodes. However, this approach requires implementing

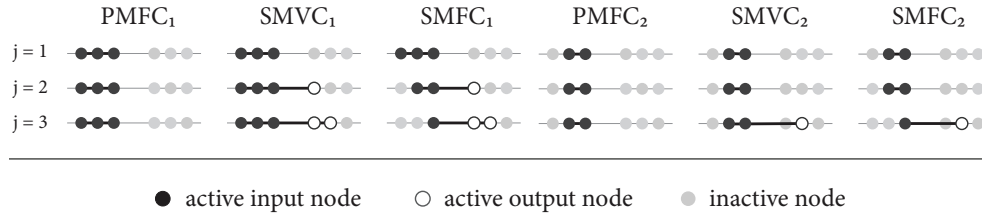


**Fig. 2:** A stencil-like diagram showcasing the three construction strategies for methods with three outputs ( $q = 3$ ) and equispaced nodes  $\{z_j\}_{j=1}^3 = \{-1, 0, 1\}$ . Each type of method must compute three outputs and therefore requires three polynomials. The stencils for each of these polynomials are stacked vertically. The horizontal gray-lines represent the time axis that flows to the right. The leftmost group of three dots on each time-line represents the input nodes while the rightmost group of three dots represent the output nodes. If the data at a node is unused then the node is colored light-gray; otherwise, the node is colored dark black if it is an input node or white if it is an output node.

a separate method. Moreover, it may not always be possible to match the order of a starting method with that of the EPBM. Here we present an alternative strategy for obtaining initial conditions by repeatedly applying an iterator method (i.e. a polynomial method with  $\alpha = 0$ , described in Section 1.3.1).

If a set of input values contains at least one accurate initial condition, then it is possible to construct a polynomial method that iteratively improves the accuracy of the other solution values [3, Chpt. 6.2]. This is accomplished by repeatedly applying a polynomial iterator method that uses the accurate value as the initial condition in a discrete Picard iteration. Each application of the method increases the order-of-accuracy of the inputs by one. The maximum achievable accuracy is bounded above by the order of the iterator or the order of the accurate initial condition. This idea is closely related to spectral deferred correction methods [9], except we do not use an error formulation and we do not discard any values after the iteration is complete.

Here we describe two exponential iterators that can be used to produce input values for any EPBM. They are both constructed using the strategies from Section 4.1. For simplicity we assume that the initial condition is given at the first node so that  $\mathbf{y}_1^{[0]} = y(rz_1 + t_0)$  (if this is not true, then simply redefine  $t_0$ ). We first obtain a coarse estimate for the remaining initial values by assuming that the solution is equal at all the nodes. We then repeatedly apply an iterator to improve the accuracy of this coarse estimate. We can abstractly write the formula for this iteration as

$$\mathbf{y}^{[0]} = M^k \mathbf{c} \qquad \mathbf{c}_j = \mathbf{y}_1^{[0]}, \quad j = 1, \dots, q,$$

where  $\mathbf{c}$  denotes the initial coarse approximation,  $M$  denotes the PBM iterator method, and the computation involves applying the method  $k$  times to the course initial condition  $\mathbf{c}$ .

To construct the method  $M$  we propose the following parameters:  $L_y^{[j]}(\tau) = L_y(\tau)$  from (4.1),  $b_j = z_1$ , and  $L_N^{[j]}(\tau)$  or  $L_R^{[j]}(\tau)$  should be constructed in accordance with the formulas for  $\text{PMFC}_\ell$  or  $\text{SMFC}_\ell$ . Selecting  $\text{PMFC}_\ell$  leads to a parallel iterator while  $\text{SMFC}_\ell$  leads to a serial iterator. The  $\text{SMVC}_\ell$  construction cannot be used since the input and output nodes overlap when  $\alpha = 0$ . For typical node choices  $\{z_j\}_{j=1}^q$  it is

sufficient to run the iteration  $q$  times, however node sets that allow for higher accuracy can benefit from additional iterations. Finally, as  $k \rightarrow \infty$  the iteration converges to the stages and outputs of a fully implicit exponential collocation method.

Iterators can also be applied to construct composite EPBMs. An iterator and a propagator that share the same nodes can be combined to create a composite method whose computation involves first advancing the timestep with the propagator and then correcting the output  $k$  times with the iterator. The composite method can be written abstractly as

$$\mathbf{y}^{[n+1]} = M^k P \mathbf{y}^{[n]}$$

where  $P$  denotes a propagator and  $M$  the iterator. As we show in our numerical experiments, this method construction can lead to methods with improved stability properties.

**4.3. Parallel methods with Legendre nodes.** The parameter choices proposed in Section 4.1 can be used to construct families of partitioned or unpartitioned exponential methods. To obtain one single method it is necessary to select a set of nodes and the extrapolation parameter  $\alpha$ .

For the sake of brevity, we only analyze parallel polynomial exponential methods where  $L_N(\tau)$  is constructed in accordance to the PMFO strategy. Furthermore we only consider nodes that are given by the union of negative one and the  $q-1$  Legendre points so that

$$(4.2) \quad \{z_j\}_{j=1}^q = \{-1, x_1, \dots, x_{q-1}\}$$

where  $x_j$  is the  $j$ th zero of the  $q$ th Legendre polynomial  $P_q(x)$ . Since we are using Legendre points we choose the PMFC<sub>2</sub> construction strategy so that the polynomials for  $L_N^{[j]}(\tau)$  or  $L_R^{[j]}(\tau)$  are both constructed using only the Legendre nodes. We also select  $b_j = z_1$  so that the integration endpoint is negative one. We describe the methods parameters in the Table 2.

$$\begin{aligned} \{z_j\}_{j=1}^q & : (4.2) \\ L_y^{[j]}(\tau) & : L_y(\tau) \text{ from (4.1)} \\ L_N^{[j]}(\tau) \text{ or } L_R^{[j]}(\tau) & : \text{PMFC}_2 \end{aligned}$$

**Table 2:** Parameters for Legendre EPBMs. The coefficients for methods with  $q = 2, 3, 4$  are shown in Appendix B.

Like all polynomial methods, these Legendre EPBMs are parametrized in terms of the extrapolation factor  $\alpha$ ; we can write the method abstractly as  $M(\alpha)$ . Different choices will impact both the method’s stability, accuracy, and susceptibility to round-off errors. We will primarily focus on Legendre propagators with  $\alpha = 2$ , and Legendre iterators with  $\alpha = 0$ . For dispersive equations we also briefly consider composite methods of the form

$$(4.3) \quad M_{\text{composite}}(\alpha) = M(0)^k M(\alpha).$$

Finally, though we have found that Legendre based nodes lead to efficient methods, they are by no means the optimal choice. However, optimal node selection is nontrivial and should be treated as a separate topic.

**5. Linear stability.** We now briefly analyze the linear stability properties of partitioned and unpartitioned Legendre EPBMs from Table 2. Like all unpartitioned integrators, any unpartitioned EPBM will integrate the classical Dahlquist test problem  $y' = \lambda y$  exactly, and therefore its linear stability region is always equal to the left-half-plane  $\text{Re}(h\lambda) \leq 0$ . To analyze linear stability for partitioned methods we use the generalized Dahlquist test problem [1, 20, 21, 7, 8, 24, 15, 36]

$$(5.1) \quad y' = \lambda_1 y + \lambda_2 y,$$

where the terms  $\lambda_1 y$  and  $\lambda_2 y$  are meant to respectively represent the linear and nonlinear terms. When applied to (5.1), an EBPM with  $q$  inputs reduces to the matrix iteration

$$\mathbf{y}_{n+1} = \mathbf{M}(z_1, z_2, \alpha) \mathbf{y}_n$$

where  $\mathbf{M}$  is a  $q \times q$  matrix,  $z_1 = h\lambda_1$ ,  $z_2 = h\lambda_2$ , and  $h$  denotes the timestep. The stability region  $S$  is the subset of  $\mathbb{C}^2 \times \mathbb{R}^+$  where  $\mathbf{M}(z_1, z_2, \alpha)$  is power bounded, so that

$$S = \left\{ z : \sup_{n \in \mathbb{N}} \|\mathbf{M}(z_1, z_2, \alpha)^n\| < \infty \right\}.$$

The matrix  $\mathbf{M}(z_1, z_2, \alpha)$  is power bounded if its eigenvalues lie inside the closed unit disk, and any eigenvalues of magnitude one are non-defective. The stability region  $S$  is five-dimensional and cannot be shown directly. Instead, we overlay two-dimensional slices of the stability regions formed by fixing  $z_1$  and  $\alpha$  while allowing  $z_2$  to vary. The choices for  $z_1$  are:

1.  $z_1 \in -1 \cdot [0, 30]$ : negative real-values mimic a problem with linear dissipation.
2.  $z_1 \in i \cdot [0, 30]$ : imaginary-values mimic a problem with linear dispersion.
3.  $z_1 \in \exp\left(\frac{3\pi i}{4}\right) \cdot [0, 30]$ : complex-values mimic both dispersion and dissipation.

We compare the linear stability regions of Legendre EPBMs to those of exponential Adams-Bashforth (EAB) [2] and the fourth-order exponential Runge-Kutta (ERK) method from [8]. It is interesting to compare EPBMs to EABs since both methods are constructed using high-order Lagrange polynomials. On the other hand, ERK methods serve as a good benchmark for gauging stability since they are stable on a variety of problems [30, 22, 8, 15].

In Figure 3 we show the stability regions for fourth and eighth order Legendre EPBMs with  $\alpha = 2$  compared against those of ERK4 and the fourth and eighth order EAB methods. In Figure 4 we also show magnified plots that highlight the stability properties near the origin.

When dissipation is present, the stability regions for EPBMs are significantly larger than those of EAB schemes. The difference between the two methods increases with order, with the eighth-order EPBM possessing a stability region that is approximately thirty-two times larger than the eighth-order EAB method for small  $|z_1|$ . For large values of  $|z_1|$ , the stability regions of EPBMs are comparable to those of the fourth-order Runge-Kutta, however, for smaller  $|z_1|$ , Runge-Kutta integrators display larger stability regions.

For the purely dispersive Dahlquist test problem, all three families of integrators have small stability regions that contract as  $|z_1|$  increases. For small  $|z_1|$  ERK has the largest stability regions, followed by EPBM, and lastly the EAB. These results

suggest that high-order EPBMs will exhibit poor stability properties for purely dispersive equations. However, we can remedy the situation by considering the composite method (4.3). In Figure 5 we plot the stability regions for the composite method with  $q = 4, 6, 8$  and  $k = 0, 1, 2$  where  $k$  is the number of times the iterator method is applied. The cost of the composite method scales by a factor of  $(k + 1)$  compared to the propagator, therefore it is critical that the stability regions increases by a similar factor or the composite method will not be as efficient as the propagator alone. Fortunately, by applying even a single iterator the linear stability properties increase drastically suggesting that composite schemes are suitable for efficiently solving dispersive equations.

Finally, since the parameter choices and plot axes in Figure 3 are identical to those presented in [4] we can also compare the stability regions of EPBMs to those of high-order exponential SDC methods constructed with Chebyshev nodes. Overall ESDC methods had significantly improved stability regions compared to all methods shown in this paper. Moreover, unlike EPBM or EAB, the stability regions of high-order ESDC methods grow with order.

**6. Numerical experiments and discussion.** We investigate the efficiency of the Legendre EPBMs from Table 2 by conducting six numerical experiments consisting of four partitioned systems and two unpartitioned systems. The systems all arise from solving partial differential equations using the method of lines. In each case, the reference solutions were computed numerically by averaging the outputs of multiple methods that were run using a small timestep.

We divide our numerical experiments and the subsequent discussion into a partitioned and unpartitioned section. In both cases we compare Legendre EPBMs against exponential Adams Bashforth (EAB) [2, 40], exponential spectral deferred correction (ESDC) [4], and the fourth-order exponential Runge-Kutta (ERK) methods from [8] and [29]. We selected EAB and ESDC schemes because both types of methods can be constructed at arbitrarily high orders-of-accuracy for both partitioned and unpartitioned problems. We also include exponential Runge-Kutta schemes since they have proven very efficient compared to a host of other methods [29, 35, 30].

We provide the code that was used to run the experiments in [5]. Furthermore, all the timing results presented in this paper were produced on a computer with a 3.7 Ghz Intel i7-8700 processor. Finally, since the equations and spatial discretizations are identical to those presented in [4], we only list the critical information for each problem below.

**6.1. Partitioned numerical experiments.** We consider the following equations that are each equipped with periodic boundary conditions:

1. The **Kuramoto-Sivashinsky** (KS) equation from [25, 22],

$$(6.1) \quad \begin{aligned} \frac{\partial u}{\partial t} &= -\frac{\partial^2 u}{\partial x^2} - \frac{\partial^4 u}{\partial x^4} - \frac{1}{2} \frac{\partial}{\partial x} (u^2), \\ u(x, t = 0) &= \cos\left(\frac{x}{16}\right) \left(1 + \sin\left(\frac{x}{16}\right)\right), \quad x \in [0, 64\pi], \end{aligned}$$

integrated to time  $t = 60$  using a 1024 point Fourier spectral discretization in  $x$ .

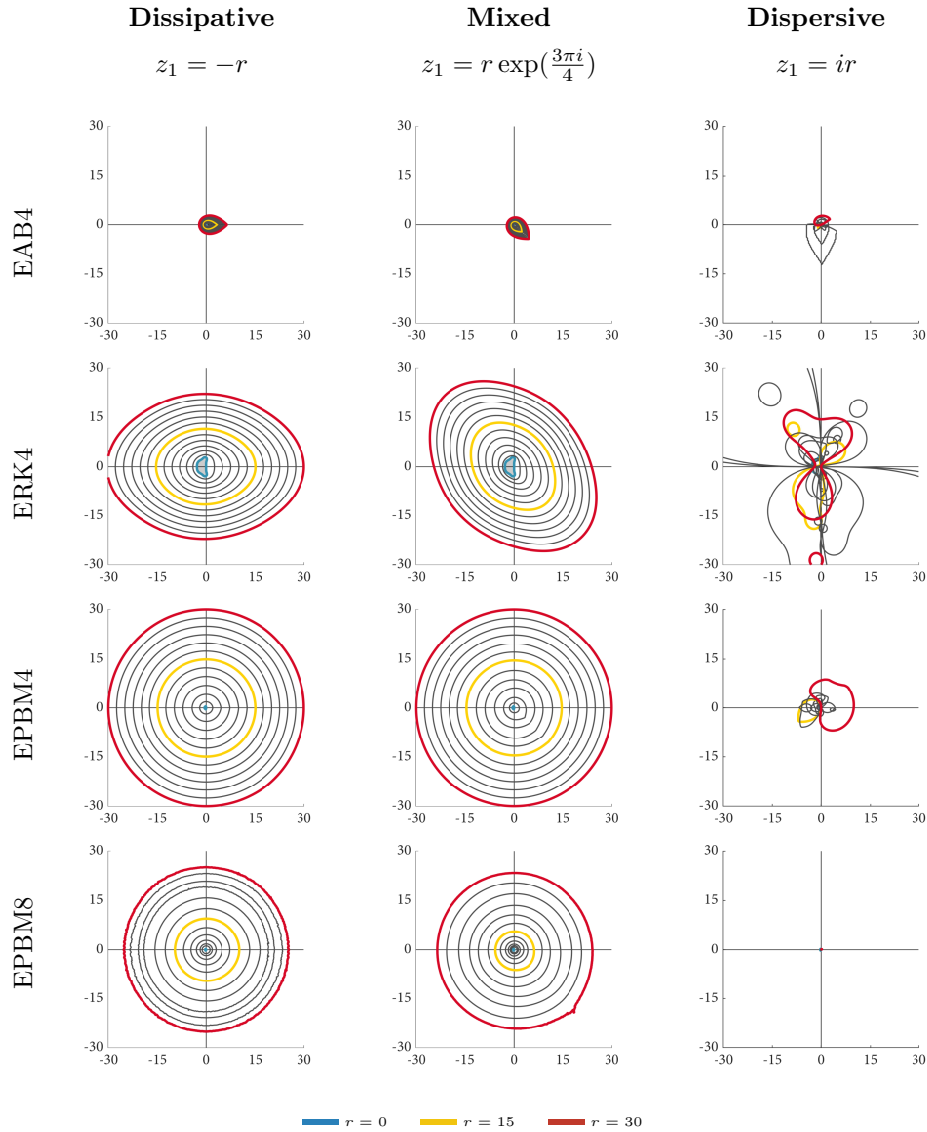


**Fig. 3:** Linear stability regions of the fourth-order EAB [2], the fourth-order ERK4 [8] and the fourth-order and eighth-order Legendre EPBMs from Table 2. Each row corresponds to a method and each column to one of the three choices for  $z_1$  described in Section 5. The colored contours represent the stability regions for  $z_1$  with magnitudes of 0, 15, and 30. We did not include the stability regions for eighth-order exponential Adams-Bashforth in this plot since they are too small to be visible at this scale.

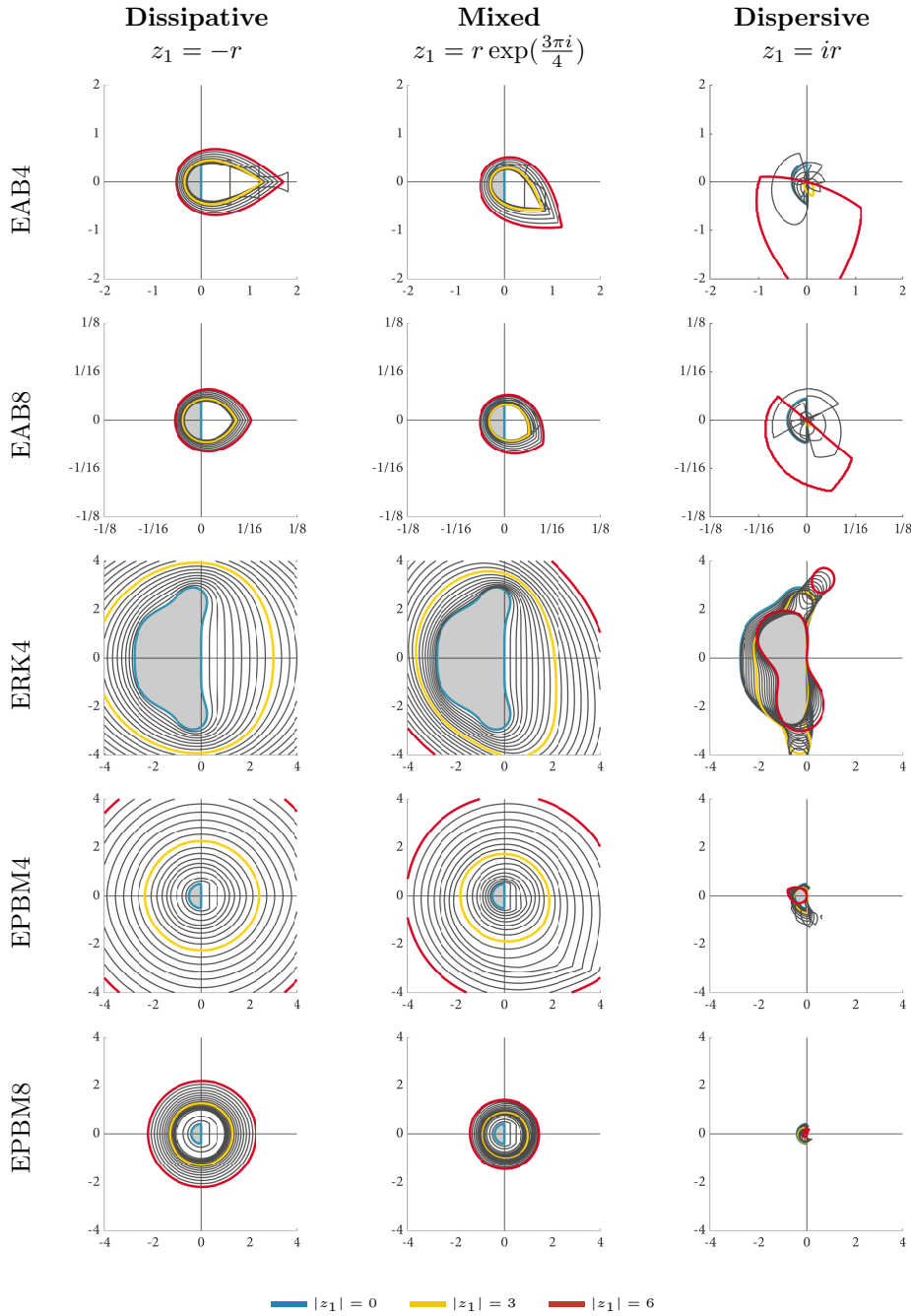


**Fig. 4:** Magnified stability regions from Figure 3. The axis used in the plots for the EAB4 and EAB8 are magnified by a factor of 2 and 32, respectively, compared to those of the ERK4 and the Legendre EPBMs. Note that the colored contours now denote stability regions where  $z_1$  has magnitude 0, 3, and 6.

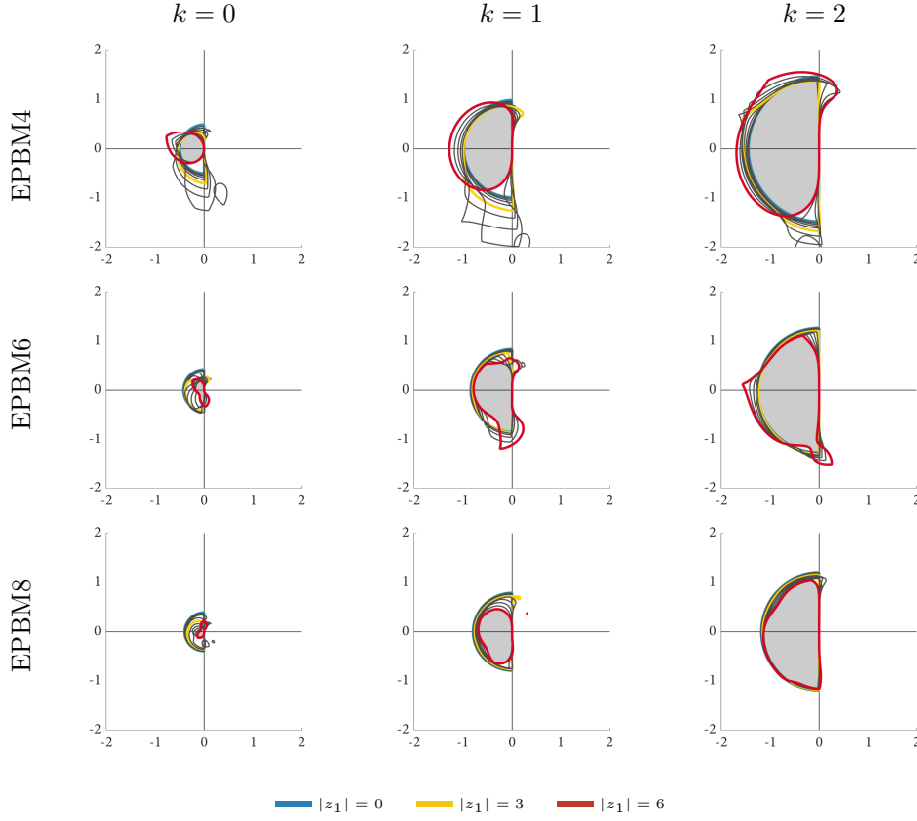


**Fig. 5:** Magnified stability regions for composite Legendre methods (4.3) on the dispersive Dahlquist test problem where  $z_1 = ir$ . The composite methods takes one propagation step with  $\alpha = 2$  and  $k$  iteration steps with  $\alpha = 0$ . The stability regions increase substantially even after a single iteration step.

2. The **Nikolaevskiy** equation from [39, 15],

$$(6.2) \quad \frac{\partial u}{\partial t} = \alpha \frac{\partial^3 u}{\partial x^3} + \beta \frac{\partial^5 u}{\partial x^5} - \frac{\partial^2}{\partial x^2} \left( r - \left( 1 + \frac{\partial^2}{\partial x^2} \right)^2 \right) u - \frac{1}{2} \frac{\partial}{\partial x} (u^2),$$

$$u(x, t = 0) = \sin(x) + \epsilon \sin\left(\frac{x}{25}\right), \quad x \in [-75\pi, 75\pi],$$

where  $r = 1/4$ ,  $\alpha = 2.1$ ,  $\beta = 0.77$ , and  $\epsilon = 1/10$ . The equation is integrated to time  $t = 50$  using a 4096 point Fourier spectral discretization.

3. The **Korteweg-de Vries** (KDV) equation from [42]

$$(6.3) \quad \frac{\partial u}{\partial t} = - \left[ \delta \frac{\partial^3 u}{\partial x^3} + \frac{1}{2} \frac{\partial}{\partial x} (u^2) \right]$$

$$u(x, t = 0) = \cos(\pi x), \quad x \in [0, 2],$$

where  $\delta = 0.022$ . This equation is integrated to time  $t = 3.6/\pi$  using a 256 point Fourier spectral discretization.

4. The **barotropic quasigeostrophic** equation on a  $\beta$ -plane with linear Ekman drag and hyperviscous diffusion of momentum from [15]:

$$(6.4) \quad \begin{aligned} \partial_t \nabla^2 \psi &= - [\beta \partial_x \psi + \epsilon \nabla^2 \psi + \nu \nabla^{10} \psi + \mathbf{u} \cdot \nabla (\nabla^2 \psi)] \\ \psi(x, y, t = 0) &= \frac{1}{8} \exp \left( -8 (2y^2 + x^2/2 - \pi/4)^2 \right), \\ (x, y) &\in [-\pi, \pi]. \end{aligned}$$

where  $\beta = 10$ ,  $\epsilon = 1/100$ ,  $\nu = 10^{-14}$ . The equation is integrated to time  $t = 5$  using a  $256 \times 256$  point Fourier discretization.

Each of these four equations are solved in Fourier space with no anti-aliasing. Since linear derivative operators diagonalize in Fourier space, we can write each initial value problem as  $\mathbf{y}' = \mathbf{L}\mathbf{y} + N(t, \mathbf{y})$  where  $\mathbf{L}$  is a diagonal operator that includes all the discretized linear derivative terms. Computing matrix-vector products with  $\varphi$ -functions of  $\mathbf{L}$  now amounts to multiplication with a diagonal matrix. Moreover, we can efficiently precompute and store the diagonal entries of  $\varphi_j(\mathbf{L})$  as a vector. For small wave numbers with magnitude less than one we compute the diagonal entries of  $\varphi_j(\mathbf{L})$  using the contour integral method [22], while for larger wave numbers we simply use the recurrence relation  $\varphi_{j+1}(z) = z^{-1}(\varphi_j(z) - 1/n)$ ,  $\varphi_0(z) = e^z$ .

One of the key features of the Legendre EPBMs is their inherent parallelism. In order to investigate the potential advantages of this approach we implemented all the schemes in Fortran and used OpenMP to parallelize the EPBM computation. In Figure 6 we present plots of relative error versus stepsize, and relative error versus computational time for each of the four partitioned problems. In Figure 7 we also investigate the efficiency EPBMs when they are implemented in serial by repeating our Kuramoto experiment without OpenMP. For the dispersive KDV equation we conduct a separate test in Figure 8 using the composite Legendre methods (4.3) in order to validate the results of the linear stability analysis. Finally, in Figure 9 we also briefly investigate the effects of varying  $\alpha$  on the Nikolaevskiy equation where high-order EPBMs showed order reduction.

**6.2. Discussion of partitioned numerical experiments.** By precomputing the matrix exponential functions, the cost of computing a matrix-vector product  $\varphi_j(\mathbf{L})\mathbf{x}$  is equivalent to that of multiplying  $\mathbf{x}$  with a diagonal matrix. Therefore, the majority of the computational work for the partitioned experiments is due to nonlinear function evaluations. Two key factors that determine a method's overall efficiency are its cost per timestep and its stability properties. If it remains stable, a method with cheaper cost per timestep will produce results faster than a more expensive method. However, if the more expensive method can take substantially larger timesteps, then it may be able to provide a stable solution in less computational time. These two factors must also be balanced with the overall accuracy of both methods.

Exponential Adams-Bashforth methods require only a single nonlinear function evaluation per timestep and serve as a benchmark for optimal performance. In contrast, Legendre EPBMs require one function evaluation per node. However, since the outputs are independent, each function evaluation can be computed in parallel. If we neglect parallel overhead, then EPBMs have the same cost per timestep as an EAB method. On the other hand an ESDC method with  $q$  nodes requires  $q(q-1)$  serial function evaluations per timestep, making the cost significantly higher than that of other methods. Finally the fourth-order Runge-Kutta method requires four serial function evaluations per timestep.

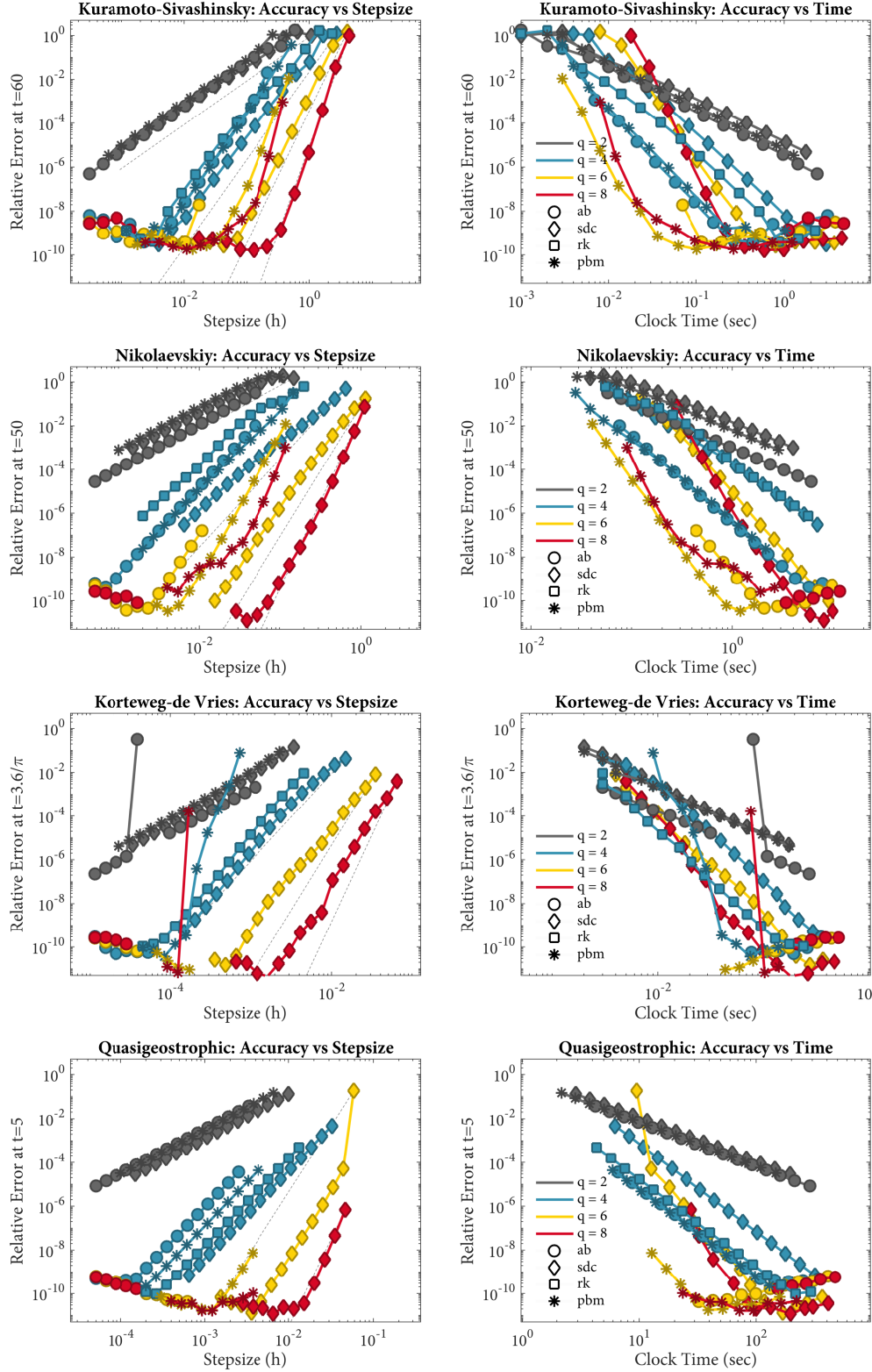


**Fig. 6:** Plots of accuracy versus stepsize and accuracy versus clock-time for the four partitioned equations. The thin, dashed gray lines in the accuracy versus stepsize plots correspond to second, fourth, sixth, and eighth order convergence.

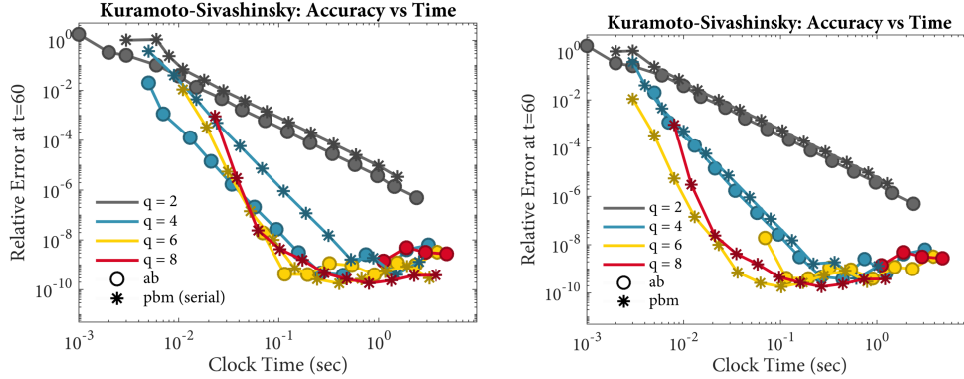


**Fig. 7:** Quantifying the effects of parallelism on the KS equation. The two plots show the accuracy versus clock time for EAB and EPBMs that are implemented in serial (left) and in parallel (right). The right plot is identical to the one shown in Figure 6 except that ESDC and ERK methods have been removed.

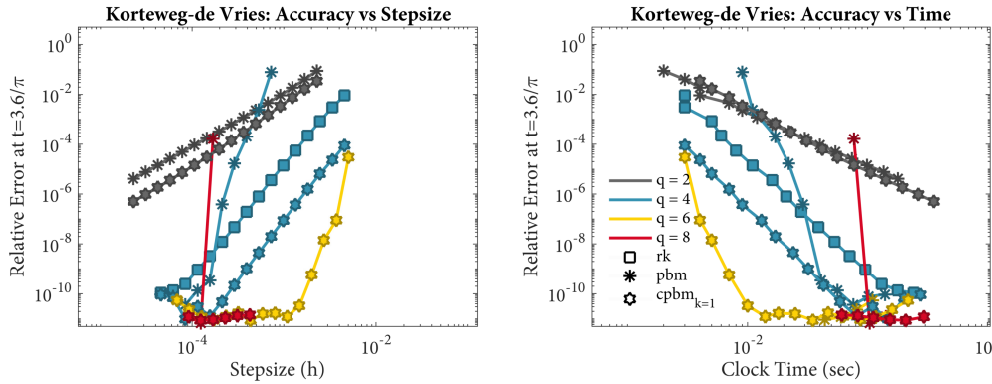


**Fig. 8:** Composite methods for solving KDV. We compare Legendre EPBMs to the composite Legendre methods (4.3) with  $k = 1$ . We also include ERK4 which was one of the most efficient methods for solving KDV in Figure 6. As suggested by the linear stability results, applying even a single iteration drastically improves the stability of the method for dispersive equations.

Our results in Figure 6 demonstrate that high-order Legendre EPBMs were able to consistently achieve the best accuracy in the smallest amount of computational time. This was due to their improved accuracy and use of parallelism. For one-dimensional problems with dissipation, EPBMs were significantly more efficient than existing methods at all but the coarsest error tolerances. Overall, EPBM8 was less efficient than EPBM6. This is likely due to two reasons. First the CPU used to run the simulation only had six cores so it was not possible to fully parallelize the eight function evaluations per timestep. Secondly, EPBM8 also showed order reduction at small timesteps, the most notably case being the Nikolaevskiy experiment. This phenomenon is due to rounding error and is present in other high-order polynomial integrators [6, 3]. As shown in Figure 9, the solution is to simply select a

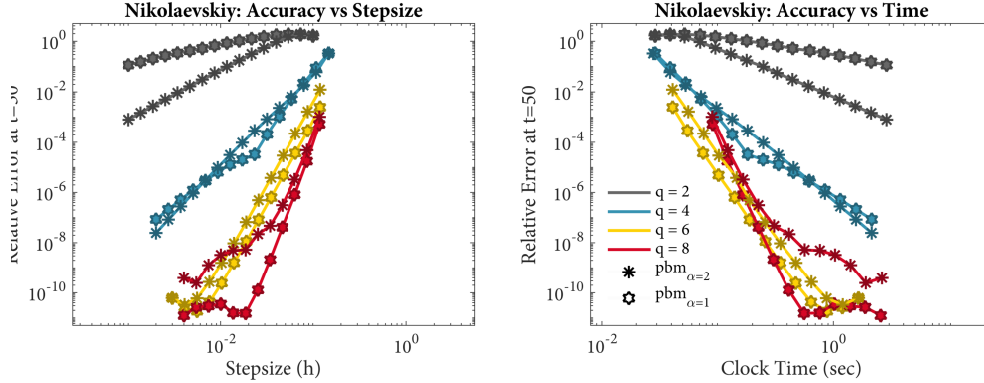


**Fig. 9:** Quantifying the effects of the extrapolation parameter  $\alpha$ . Accuracy versus stepsize and accuracy versus clock time for the Nikolaevskiy equation using Legendre EPBMs with  $\alpha = 2$  and  $\alpha = 1$ . High-order methods benefit from a smaller  $\alpha$  to avoid problems with round-off errors, however low order methods have better error constants with larger  $\alpha$ .

smaller extrapolation factor, after which EPBM8 becomes the most efficient method for obtaining highly accurate solutions.

When EPBMs were run in serial on the Kuramoto equation (Figure 7), their computational advantages decreased significantly and they only marginally outperformed EAB schemes at low error tolerances. This occurs because a serial implementation of a Legendre method with  $q$  nodes requires  $q - 1$  function evaluations per timestep, compared to the single function evaluation for an AB scheme. Parallelization overhead also caused significant degradation in the EPBMs performance on the two-dimensional quasigeostrophic equation. This is evident from the large differences in running time of EPBMs of different orders. For example, all the EPBMs converged at a timestep of  $3.5 \times 10^{-3}$ . Ignoring any parallel overhead, the cost of running an EPBM of any order should be identical. However, each increase in order increased the computational time by a factor of two. It is apparent that the CPU was not able to efficiently compute multiple two-dimensional Fourier transforms in parallel.

Finally, as predicted by linear stability analysis, Legendre EPBMs demonstrated poor stability on the dissipative KDV equation and only converged at smaller timesteps. However, the composite Legendre method with  $k = 1$  shown in Figure 8 was able to retain stability across a much wider range of timesteps. Moreover, though its cost per timestep is twice that of a standard EPBM, the improved stability and accuracy allowed it to be performed significantly more efficiently than any of the other methods on the KDV equation.

**6.3. Unpartitioned initial value problems.** We consider the two dimensional ADR equation with homogeneous Neumann boundary conditions from [35],

$$(6.5) \quad \begin{aligned} u_t &= \epsilon(u_{xx} + u_{yy}) + \delta(u_x + u_y) + \gamma u(u - 1/2)(1 - u), \\ u(x, t = 0) &= 256(xy(1 - x)(1 - y))^2 + 0.3 \\ x, y &\in [0, 1]. \end{aligned}$$

The equation is integrated to time  $t = 1/100$  and the spatial discretization employs standard second-order accurate finite differences on a  $200 \times 200$  point grid. We solve this equation using the two parameters sets described in Table 3 which lead to either a stiff linearity or a stiff nonlinearity.

|                    | $\epsilon$ | $\delta$ | $\gamma$ | $\rho(\mathbf{L})$ | $\rho\left(\frac{\partial N}{\partial y}\right)$ |
|--------------------|------------|----------|----------|--------------------|--|
| stiff linearity    | 1/100      | -10      | 100      | 4288               | 167  |
| stiff nonlinearity | 1/10000    | -1/10    | 1000     | 43                 | 1670   |

**Table 3:** Two set of parameters for the 2D ADR equation. We also show the spectral radius  $\rho$  for the linear and nonlinear terms.

To compute matrix-vector products with  $\varphi$ -functions we apply the Krylov-based KIOPs algorithm [13] using the exact Jacobian. In Figure 10 we show results for Legendre EPBMs of orders two, four, six and eight compared against unpartitioned Adams-Bashforth methods [40], unpartitioned exponential spectral deferred correction [4], and the fourth-order unpartitioned exponential Runge-Kutta method EPIRK43s [29].

**6.3.1. Discussion of unpartitioned numerical experiments.** All unpartitioned exponential integrators require matrix-vector products with  $\varphi$ -functions of the Jacobian. Since the Jacobian varies in time, we are no longer able to store the exponential matrix functions at the first time step. Moreover, the Jacobian matrices are non-diagonal, therefore the majority of the computational effort at each time step is now due to the vector products with  $\varphi$ -functions.

Krylov methods like KIOPS [13] and PHIPM [32, 31] approximate matrix-vector products of  $\varphi$ -functions within a Krylov subspace. The operation to build a Krylov space and approximate a  $\varphi$ -function is called a *projection* and its cost will depend on the spectrum of  $\mathbf{A}$ . The cost of a time-integrator is therefore dependent on the total number of projections per time step. In general, every  $\varphi$ -function in an arbitrary linear combination must be computed using a separate projection. However, expressions of the form

$$(6.6) \quad \varphi_0(\tau\mathbf{A})\mathbf{x}_0 + \tau\varphi_1(\tau\mathbf{A})\mathbf{x}_1 + \tau^2\varphi_2(\tau\mathbf{A})\mathbf{x}_2 + \dots + \tau^p\varphi_p(\tau\mathbf{A})\mathbf{x}_p$$

can be evaluated at multiple  $\tau$  values in a single projection. Furthermore this computation is made cheaper if  $\tau$  is small. This fact can be used to construct highly efficient integrators such as EPIRK methods [40, 41, 35, 29] whose coefficients are specifically chosen to minimize the total number of projections required at each timestep.

All polynomial  $\varphi$ -expansions can be written in the form (6.6) and therefore each output of any EPBM requires only one projection to compute. Moreover, since Legendre EPBMs are constructed using a single Adams polynomial  $\varphi$ -expansion, all the outputs can be computed in one projection where  $\tau = 2h$ . In comparison EPIRK4s requires two serial projections: the first from  $\tau = h$  and the second where  $\tau = h/9$ . Exponential Adams-Bashforth methods once again serve as a benchmark for optimal cost per timestep as they only require one projection where  $\tau = h$ . ESDC methods are the most expensive requiring one projection per correction iteration, meaning that a method with  $q$  nodes requires  $q$  projections.

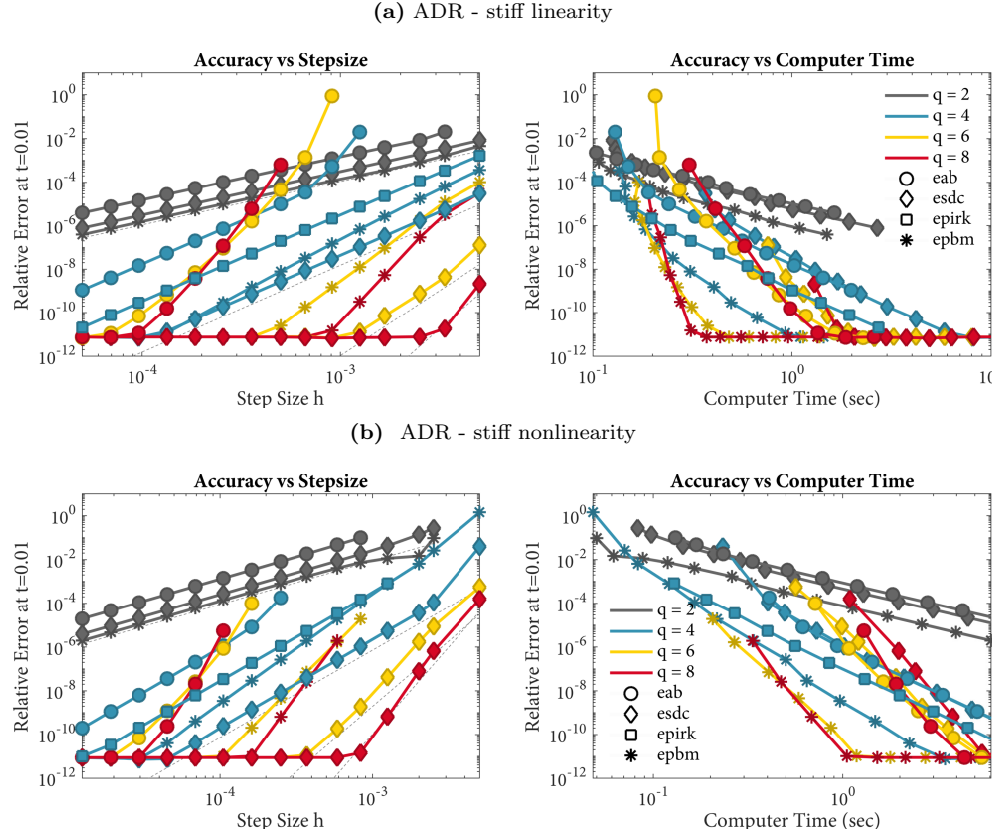


**Fig. 10:** (a) Diagrams for the ADR equation with a stiff linearity. (b) Diagrams for the ADR equation with a stiff nonlinearity. The dashed lines in the accuracy diagrams correspond to second, fourth, sixth and eighth order convergence.

For unpartitioned Legendre EPBMs it is also possible to parallelize the right-hand-side evaluations. However, for our test problems the cost of right-hand-side evaluations of  $R(\mathbf{y})$  is negligible compared to that of the Krylov projections. Under these conditions, the cost per timestep of an unpartitioned Legendre EPBM can be up to roughly twice as expensive as EPIRK43s and EAB methods, and a factor of  $q/2$  times less expensive than an ESDC method with  $q$  nodes. Despite the increased cost per timestep, the high-order of accuracy of EPBMs allow them to be significantly more efficient than the EPIRK43s, EAB, and ESDC methods at nearly all error tolerances. Overall, EPBMs also demonstrated significantly improved error constants compared to EAB methods of the same order.

Finally we note that it is trivial to construct methods that only require a projection with  $\tau = h$  per timestep. For example, we obtain this property by choosing Chebyshev nodes and PMFO<sub>1</sub> with endpoints  $b_j = 1$ . It is also simple to apply parallelism to speed up the computation of methods that use different endpoints  $b_j$  or polynomials  $L_R^{[j]}(\tau)$  for computing each output. Though such methods will require  $q$  projections per timestep, each projection can now be computed in parallel to nullify the additional cost.

**7. Summary and Conclusions.** We presented an extension of the polynomial framework that incorporates exponential integration. To achieve this we combined the classical ODE polynomial with the integrating factor method to introduce the polynomial  $\varphi$ -expansions that form the basis of the new methods. By utilizing polynomial  $\varphi$ -expansions it is possible to construct many families of new exponential integrators including those with desirable properties such as parallelism and high-order.

After introducing the framework we demonstrated its potential by presenting several general construction strategies for EPBMs and by deriving a new class of parallel EPBMs that use Legendre points. Our numerical experiments demonstrate the potential of these new parallel methods for both partitioned and unpartitioned problems. Based on our results it appears that Legendre EPBMs can provide significant computational savings compared to current state-of-the-art methods if they can be efficiently parallelized.

The generality of the exponential polynomial framework creates many opportunities for additional developments that we plan to address in future work. In particular we will investigate the construction of exponential polynomial general linear methods that can exploit parallelism on a larger scale. There are also many additional opportunities for deriving EPBMs with optimized parameters that will be more efficient than those presented in this work.

**8. Acknowledgments.** I would like to thank Randall LeVeque for encouraging me to develop polynomial integrators during my graduate studies and for his comments and guidance through the course of this project. I would also like to thank Mayya Tokman for sharing her vast knowledge about exponential integrators and for her helpful comments on drafts of this work.



**Appendix A. Equivalent representations for polynomial  $\varphi$ -expansions.**

Here we show that the three formulas presented in Definition 3.3 are equivalent. First, by applying the integrating factor method with  $\exp(-\mathbf{L}t)$  to (3.5) we obtain (3.4). Next we substitute the definition for the ODE polynomial (3.2) into the integral in (3.4) to obtain

$$\int_{b_3}^{\tau} e^{r\mathbf{L}(\tau-s)} \sum_{j=0}^g \frac{a_j(b_2)(s-b_2)^j}{j!} ds.$$

Making the change of variables  $s = (\tau - b_3)\nu + b_3$  leads to

$$h(\tau) \int_0^1 e^{rh(\tau)\mathbf{L}(1-s)} \sum_{j=0}^g \frac{a_j(b_2)(h(\tau)s - c)^j}{j!} ds,$$

where  $h(\tau) = (\tau - b_3)$  and  $c = b_3 - b_2$ . Finally, using the binomial theorem we have

$$\begin{aligned}
& h(\tau) \int_0^1 e^{rh(\tau)\mathbf{L}(1-s)} \sum_{j=0}^g \frac{a_j(b_2)}{j!} \sum_{k=0}^j \binom{j}{k} (h(\tau)s)^k c^{j-k} ds \\
&= h(\tau) \int_0^1 e^{rh(\tau)\mathbf{L}(1-s)} \sum_{k=0}^g s^k \sum_{j=k}^g \frac{a_j(b_2)}{j!} \binom{j}{k} h(\tau)^k c^{j-k} ds \\
&= h(\tau) \int_0^1 e^{rh(\tau)\mathbf{L}(1-s)} \sum_{k=0}^g \frac{s^k}{k!} \mathbf{c}_k(\tau) ds \quad \text{for} \quad \mathbf{c}_k(\tau) = \sum_{j=k}^g \frac{a_j(b_2)h(\tau)^k c^{j-k}}{(j-k)!} \\
&= h(\tau) \sum_{k=0}^g \mathbf{c}_k(\tau) \varphi_{k+1}(rh(\tau)\mathbf{L}).
\end{aligned}$$

### Appendix B. Method Coefficients.

The general form for a Legendre method from Table 2 with  $q$  nodes is

$$y_j^{[n+1]} = \varphi_0(r\eta_j\mathbf{L})y_1^{[n]} + r \sum_{k=1}^{q-1} \eta_j^k \varphi_k(r\eta_j\mathbf{L})\mathbf{v}_j, \quad j = 1, \dots, q,$$

where  $\eta_j = z_j + \alpha + 1$  and  $\mathbf{N}_j = N(z_j, \mathbf{y}(z_j))$ . The vectors  $\mathbf{v}_j$  for can be derived by computing the derivatives of the Lagrange polynomial

$$L(\tau) = \sum_{j=1}^{q-1} \ell_j(\tau)\mathbf{N}_j, \quad \ell_j(\tau) = \prod_{\substack{l=1 \\ l \neq j}}^{q-1} \frac{\tau - x_l}{x_j - x_l},$$

at the point  $\tau = -1$ , where  $x_j$  is the  $j$ th zero of the  $q$ th Legendre polynomial  $P_q(x)$ . Below we provide several formulas for the  $\mathbf{v}_j$  if  $q = 2, 3, 4$ .

**Legendre Method:**  $q = 2, z_j = \{-1, 0\}$

$$\mathbf{v}_1 = \mathbf{N}_2$$

**Legendre Method:**  $q = 3, z_j = \left\{-1, -\sqrt{\frac{1}{3}}, \sqrt{\frac{1}{3}}\right\}$

$$\mathbf{v}_1 = \frac{(1 + \sqrt{3})\mathbf{N}_2}{2} + \frac{(1 - \sqrt{3})\mathbf{N}_3}{2}$$

$$\mathbf{v}_2 = \frac{\sqrt{3}\mathbf{N}_3}{2} - \frac{\sqrt{3}\mathbf{N}_2}{2}$$

**Legendre Method:**  $q = 4, \{z_j\} = \left\{-1, -\sqrt{\frac{3}{5}}, 0, \sqrt{\frac{3}{5}}\right\}$

$$\mathbf{v}_1 = \frac{(5 + \sqrt{15})\mathbf{N}_2}{6} - \frac{2\mathbf{N}_3}{3} - \frac{(\sqrt{15} - 5)\mathbf{N}_4}{6}$$

$$\mathbf{v}_2 = \frac{(-10 - \sqrt{15})\mathbf{N}_2}{6} + \frac{10\mathbf{N}_2}{3} + \frac{(\sqrt{15} - 10)\mathbf{N}_4}{6}$$

$$\mathbf{v}_3 = \frac{5\mathbf{N}_2}{3} - \frac{10\mathbf{N}_3}{3} + \frac{5\mathbf{N}_4}{3}$$

## REFERENCES

- [1] U. M. ASCHER, S. J. RUUTH, AND B. T. WETTON, *Implicit-explicit methods for time-dependent partial differential equations*, SIAM Journal on Numerical Analysis, 32 (1995), pp. 797–823.
- [2] G. BEYLKIN, J. M. KEISER, AND L. VOZOVOI, *A new class of time discretization schemes for the solution of nonlinear PDEs*, Journal of Computational Physics, 147 (1998), pp. 362–387.
- [3] T. BUVOLI, *Polynomial-Based Methods for Time-Integration*, PhD thesis, 2018.
- [4] T. BUVOLI, *A class of exponential integrators based on spectral deferred correction*, SIAM Journal on Scientific Computing, 42 (2020), pp. A1–A27.
- [5] T. BUVOLI, *Codebase for Exponential Polynomial Methods*, (2020), <https://github.com/buvoli/epbm>.
- [6] T. BUVOLI AND M. TOKMAN, *Constructing new time integrators using interpolating polynomials*, SIAM Journal on Scientific Computing, 41 (2019), pp. A2911–A2937.
- [7] A. CARDONE, Z. JACKIEWICZ, A. SANDU, AND H. ZHANG, *Construction of highly stable implicit-explicit general linear methods*, Conference Publications, 2015.
- [8] S. M. COX AND P. C. MATTHEWS, *Exponential time differencing for stiff systems*, Journal of Computational Physics, 176 (2002), pp. 430–455.
- [9] A. DUTT, L. GREENGARD, AND V. ROKHLIN, *Spectral deferred correction methods for ordinary differential equations*, BIT Numerical Mathematics, 40 (2000), pp. 241–266.
- [10] B. FORNBERG, *Generation of finite difference formulas on arbitrarily spaced grids*, Mathematics of Computation, 51 (1988), pp. 699–706.
- [11] B. FORNBERG, *Calculation of weights in finite difference formulas*, SIAM review, 40 (1998), pp. 685–691.
- [12] M. J. GANDER, *50 years of time parallel time integration*, in Multiple Shooting and Time Domain Decomposition Methods, Springer, 2015, pp. 69–113.
- [13] S. GAUDREAU, G. RAINWATER, AND M. TOKMAN, *KIOPS: A fast adaptive Krylov subspace solver for exponential integrators*, Journal of Computational Physics, 372 (2018), pp. 236–255.
- [14] C. W. GEAR, *Parallel methods for ordinary differential equations*, Calcolo, 25 (1988), pp. 1–20.
- [15] I. GROOMS AND K. JULIEN, *Linearly implicit methods for nonlinear PDEs with linear dispersion and dissipation*, Journal of Computational Physics, 230 (2011), pp. 3630–3650.
- [16] T. HAUT, T. BABB, P. MARTINSSON, AND B. WINGATE, *A high-order time-parallel scheme for solving wave propagation problems via the direct construction of an approximate time-evolution operator*, IMA Journal of Numerical Analysis, 36 (2015), pp. 688–716.
- [17] M. HOCHBRUCK AND A. OSTERMANN, *Explicit exponential Runge–Kutta methods for semilinear parabolic problems*, SIAM Journal on Numerical Analysis, 43 (2005), pp. 1069–1090.
- [18] M. HOCHBRUCK AND A. OSTERMANN, *Exponential Runge–Kutta methods for parabolic problems*, Applied Numerical Mathematics, 53 (2005), pp. 323–339.
- [19] M. HOCHBRUCK AND A. OSTERMANN, *Exponential integrators*, Acta Numerica, 19 (2010), pp. 209–286.
- [20] G. IZZO AND Z. JACKIEWICZ, *Highly stable implicit–explicit Runge–Kutta methods*, Applied Numerical Mathematics, 113 (2017), pp. 71–92.
- [21] Z. JACKIEWICZ AND H. MITTELMANN, *Construction of IMEX DIMSIMs of high order and stage order*, Applied Numerical Mathematics, 121 (2017), pp. 234–248.
- [22] A. KASSAM AND L. TREFETHEN, *Fourth-order time stepping for stiff PDEs*, SIAM J. Sci. Comput., 26 (2005), pp. 1214–1233.
- [23] S. KOIKARI, *Rooted tree analysis of Runge–Kutta methods with exact treatment of linear terms*, Journal of computational and applied mathematics, 177 (2005), pp. 427–453.
- [24] S. KROGSTAD, *Generalized integrating factor methods for stiff PDEs*, Journal of Computational Physics, 203 (2005), pp. 72–88.
- [25] Y. KURAMOTO AND T. TSUZUKI, *Persistent propagation of concentration waves in dissipative media far from thermal equilibrium*, Progress of theoretical physics, 55 (1976), pp. 356–369.
- [26] J. LOFFELD AND M. TOKMAN, *Comparative performance of exponential, implicit, and explicit integrators for stiff systems of ODEs*, Journal of Computational and Applied Mathematics, 241 (2013), pp. 45–67.
- [27] J. LOFFELD AND M. TOKMAN, *Implementation of parallel adaptive-krylov exponential solvers for stiff problems*, SIAM Journal on Scientific Computing, 36 (2014), pp. C591–C616.
- [28] V. T. LUAN AND A. OSTERMANN, *Parallel exponential rosenbrock methods*, Computers & Mathematics with Applications, 71 (2016), pp. 1137–1150.
- [29] D. L. MICHELS, V. T. LUAN, AND M. TOKMAN, *A stiffly accurate integrator for elastodynamic problems*, ACM Transactions on Graphics, 36 (2017), p. 116.
- [30] H. MONTANELLI AND N. BOOTLAND, *Solving periodic semilinear stiff PDEs in 1D, 2D and 3D*

- with exponential integrators*, arXiv preprint arXiv:1604.08900, (2016).
- [31] J. NIESEN AND W. M. WRIGHT, *A Krylov subspace method for option pricing*, (2011), <http://dx.doi.org/10.2139/ssrn.1799124>.
  - [32] J. NIESEN AND W. M. WRIGHT, *Algorithm 919: A Krylov subspace algorithm for evaluating the  $\varphi$ -functions appearing in exponential integrators*, ACM Trans. Math. Softw., 38 (2012), pp. 22:1–22:19.
  - [33] A. OSTERMANN, M. THALHAMMER, AND W. M. WRIGHT, *A class of explicit exponential general linear methods*, BIT Numerical Mathematics, 46 (2006), pp. 409–431.
  - [34] G. RAINWATER AND M. TOKMAN, *A new class of split exponential propagation iterative methods of Runge–Kutta type (sEPIRK) for semilinear systems of ODEs*, Journal of Computational Physics, 269 (2014), pp. 40–60.
  - [35] G. RAINWATER AND M. TOKMAN, *A new approach to constructing efficient stiffly accurate EPIRK methods*, Journal of Computational Physics, 323 (2016), pp. 283–309.
  - [36] A. SANDU AND M. GÜNTHER, *A generalized-structure approach to additive Runge–Kutta methods*, SIAM Journal on Numerical Analysis, 53 (2015), pp. 17–42.
  - [37] M. SCHREIBER AND R. LOFT, *A parallel time integrator for solving the linearized shallow water equations on the rotating sphere*, Numerical Linear Algebra with Applications, 26 (2019), p. e2220.
  - [38] M. SCHREIBER, N. SCHAEFFER, AND R. LOFT, *Exponential integrators with parallel-in-time rational approximations for the shallow-water equations on the rotating sphere*, Parallel Computing, 85 (2019), pp. 56–65.
  - [39] E. SIMBAWA, P. C. MATTHEWS, AND S. M. COX, *Nikolaevskiy equation with dispersion*, Physical Review E, 81 (2010), p. 036220.
  - [40] M. TOKMAN, *Efficient integration of large stiff systems of ODEs with exponential propagation iterative (EPI) methods*, Journal of Computational Physics, 213 (2006), pp. 748–776.
  - [41] M. TOKMAN, *A new class of exponential propagation iterative methods of Runge–Kutta type (EPIRK)*, Journal of Computational Physics, 230 (2011), pp. 8762–8778.
  - [42] N. J. ZABUSKY AND M. D. KRUSKAL, *Interaction of solitons in a collisionless plasma and the recurrence of initial states*, Phys. Rev. Lett, 15 (1965), pp. 240–243.